ADAPTIVE TIME STEPPING IN ELASTOPLASTICITY

Dedicated to Alexander Mielke on the occasion of his 60th birthday

Sören Bartels and Jakob Keck

Department of Applied Mathematics
Mathematical Institute, University of Freiburg
Hermann-Herder-Str. 10, 79104 Freiburg i. Br., Germany

Abstract. Using rate-independant evolutions as a framework for elastoplasticity, an a posteriori bound for the error introduced by time stepping is established. A time adaptive algorithm is devised and tested in comparison to a method with constant time steps. Experiments show that a significant error reduction can be obtained using variable time steps.

1. **Introduction.** Adaptive algorithms are a common way to optimize the efficiency of numerical approximation methods. Correctly applied, they can reduce computation time and amount of data to store, or minimize these factors while not surpassing a prescribed approximation error.

In the case of elastoplasticity, several ways to implement adaptivity are known, e.g. [2, 14, 12, 17]. They mostly focus on space adaptive methods, where the triangulation for a finite element approximation is locally refined or coarsened based on a specific a posteriori error estimate. Time adaptivity on the other hand is rarely discussed. This is mainly caused by the fact, that the space discretization appears to be a more impactful source of approximation error and computation time, when compared to time discretization.

However, due to the one-dimensional nature of time, adaptivity in this one dimension is relatively easy to implement once a reasonable refinement indicator is found. Additionally, it may be possible to combine space and time adaptivity from different estimates, even though we are currently not aware of an obvious way to accomplish this.

A posteriori error estimates that simultaneously control space and time discretization errors can be obtained by formulating the evolution problem as a minimization problem in space and time, cf. [5, 15, 4]. Since these estimates do not arise as sums of local contributions it is unclear how to employ them efficiently for local mesh refinement. To our knowledge, no rigorous attempt has been made to develop adaptive time stepping methods for elastoplasticity, that is based on an estimate which exclusively focuses on the error introduced by time discretization.

Following [13] and [6] a common way to formulate linearized elastoplasticity leads
to the relations

$$-\operatorname{div}\sigma = f, \qquad \sigma = \mathbb{C}(\varepsilon(u) - p), \qquad \dot{P} \in \partial I_S(\Sigma) \qquad (1)$$

for the displacement u, stresses σ and plastic strain p, complemented by boundary
and initial conditions. The fields Σ and P are generalized versions of σ and p
respectively, that also include inner variables to control hardening; $\dot{P}$ denotes the
time derivative of P. The set of admissible stresses S is commonly obtained via
a von-Mises or Tresca yield criterion and ∂I_S denotes the subdifferential of the
indicator functional of S.

To derive a weak formulation, we let $\mathbb{R}^{d \times d}_{\text{sym}}$ denote the set of symmetric marices and
define the Hilbert space

$$Y = H^1_D(\Omega, \mathbb{R}^d) \times L^2(\Omega, \mathbb{R}^{d \times d}_{\text{sym}}) \times L^2(\Omega)$$

as well as the mappings

$$\mathcal{A}(y, w) = \int_\Omega \mathbb{C}(\varepsilon(u) - p) : (\varepsilon(v) - q) + \mathbb{H}_{\text{kin}} p : q + \mathbb{H}_{\text{iso}} ae \, dx,$$

$$\langle \ell(t), w \rangle = \int_{\Gamma_N} g(t) \cdot v \, ds + \int_\Omega f(t) \cdot v \, dx,$$

$$\Psi(y) = \int_\Omega I_S^*(p, a) \, dx,$$

with $y = (u, p, a) \in Y$ and $w = (v, q, e) \in Y$. As discussed in [6] and [9], the
conditions in (1) are then equivalent to

$$\mathcal{A}(y, w - \dot{y}) + \Psi(w) - \Psi(\dot{y}) \geq \ell(w - \dot{y}) \qquad (2)$$

for all $t \in [0, T]$ and $w \in Y$. By replacing the time derivatives in (2) with backward
difference quotients, it is possible to introduce a time discrete problem, that uniquely
defines iterates $(y^k)_{k=0,...,K}$ via the recursion

$$\mathcal{A}(y^k, w - d_t y^k) + \Psi(w) - \Psi(d_t y^k) \geq \ell^k(w - d_t y^k) \qquad (3)$$

for all $w \in Y$ and $k = 1, ...K$. Space discretization is obtained by substituting Y
with a finite element space Y_h in (2) and (3).

If y_h and $(y_h^k)_{k=0,...,K}$ are solutions of the semi-discrete problem in space and the
fully discrete problem, respectively, and $\widehat{y}_{\tau,h}$ is the piecewise affine interpolant of
(y_h^k), results of [11] and [3] lead to an a posteriori estimate of the form

$$\sup_{t \in [0,T]} ||y_h - \widehat{y}_{\tau,h}||^2_\mathcal{A} \leq 8 \sum_{k=1}^K \tau_k \varepsilon_k + 2 \sup_{t \in [0,T]} ||A_h^{-1}(\ell - \widehat{\ell}_\tau)||^2_\mathcal{A}$$

$$+ 8T \sum_{k=1}^K \tau_k^3 \sup_{t \in [t_{k-1}, t_k]} ||A_h^{-1}(\partial_{tt}^2 \ell)||^2_\mathcal{A},$$

where τ_k is the length of the k-th time interval and ε_k is a residual term that only
depends on the computed solution and can be evaluated explicitly. If the boundary
and volume forces are linearly dependent on time, the data approximation errors
responsible for the second and third term on the right-hand side of the estimate
vanish. In a more general setting, additional computation for the inversion of A_h,
which is a linear operator linked to $\mathcal{A}$, is required. We thus obtain a computable

upper bound that consists of local contributions which are used as refinement indicators for a time adaptive method.

For all the examples we use in our numerical tests, the adaptive algorithm reduces the error introduced by time discretization, when compared to a method using a similar amount of constant time steps. The reduction can be significant even for smooth data.

The outline of this paper is as follows. In Section 2 we introduce the mathematical framework, in which we establish an a posteriori error estimate. These findings are applied to elastoplasticity and further developed in Section 3. Section 4 derives a time adaptive algorithm, which is numerically tested in Section 5.

2. **Model problem and a posteriori error control.** In this section, we consider a general rate-independent evolution problem, that is used as a framework for the formulation of the elastoplastic model problem. Additionally, we develop the a posteriori estimate required for an adaptive algorithm using variable time steps. It is based on the proof of an estimate given in [3] using a general concept of [11].

Let $T > 0$, Y be a Hilbert space, $y^0 \in Y$, $\mathcal{A} : Y \times Y \to \mathbb{R}$ a continuous, symmetric and coercive bilinear form and $\ell \in W^{2,\infty}([0,T]; Y')$. We also assume, that $\Psi : Y \to \mathbb{R} \cup \{+\infty\}$ is a proper, convex and lower semicontinuous functional that is homogeneous of degree one. Using dots to denote time derivatives, the aforementioned evolution problem proposed in [6, 9] reads as follows.

Definition 2.1 (Continuous evolution)**.** Seek $y : [0,T] \to Y$, such that $y(0) = y^0$ and

$$\mathcal{A}(y, w - \dot{y}) + \Psi(w) - \Psi(\dot{y}) \geq \ell(w - \dot{y})$$

for all $t \in [0,T]$ and $w \in Y$.

Note that Y can be finite or infinite dimensional. To formulate a time discrete problem, we let $K \in \mathbb{N}$ be the number of time steps and $0 = t_0 < t_1 < ... < t_K = T$. For $k = 1, ..., K$ the length of the corresponding time step is denoted by $\tau_k = t_k - t_{k-1}$ and we use the notation $\ell^k = \ell(t_k)$ as well as the backward difference quotient d_t, i.e.

$$d_t y^k = \frac{y^k - y^{k-1}}{\tau_k}.$$

Time discretzation is introduced by replacing the time derivatives in (2.1) with backward difference quotients.

Definition 2.2 (Time stepping)**.** Seek $(y^k)_{k=1,...,K} \subset Y$, such that

$$\mathcal{A}(y^k, w - d_t y^k) + \Psi(w) - \Psi(d_t y^k) \geq \ell^k(w - d_t y^k)$$

for all $w \in Y$ and $k = 1, ...K$.

As discussed in [10], Chapter 11, both problems have unique solutions and the solution y of the continuous problem meets the regularity condition $y \in W^{1,\infty}([0,T]; Y)$. For spatial regularity properties of solutions we refer the reader to [8].

Introducing the linear, bounded and invertible operator $A : Y \to Y'$ via $\langle Av, w \rangle = \mathcal{A}(v, w)$ for $v, w \in Y$, we note, that the variational inequality in the continuous problem is equivalent to the inclusion

$$-Ay + \ell \in \partial\Psi(\dot{y}). \tag{4}$$

Defining $C_* := \partial\Psi(0)$, and considering the fact that Ψ is homogeneous of degree one, we have $\Psi = I_{C_*}^*$, where $I_{C_*}^*$ is the Legendre transform of the indicator functional of the set C_*. Additionally, convex duality relations yield the equivalence of the inclusions (4) and

$$\dot{y} \in \partial I_{C_*}(-Ay + \ell).$$

Introducing the variables $z := -y + A^{-1}\ell$ and $r := A^{-1}\dot{\ell}$ leads to

$$-\dot{z} + r \in \partial I_{C_*}(Az).$$

In the time discrete case, we proceed similarly and obtain the inclusions

$$-d_t z^k + r^k \in \partial I_{C_*}(Az^k),$$

where the transformations $z^k := -y^k + A^{-1}\ell^k$ and $r^k = A^{-1}d_t\ell^k$ are used. The monotone inclusions provide a structure that leads to an error estimate derived in [11, 3]. We provide a proof with variable time steps.

Theorem 2.3. *Suppose that $z \in W^{1,\infty}([0,T];Y)$ meets the condition*

$$-\dot{z} + r \in \partial I_{C_*}(Az),$$

for all $t \in [0,T]$ and the sequence $(z^k)_{k=0,...,K} \subset Y$ satisfies $z^0 = z(0)$ and

$$-d_t z^k + r^k \in \partial I_{C_*}(Az^k)$$

for all $k = 1,...,K$. Additionally, let $\widehat{z}_\tau : [0,T] \to Y$ denote the piecewise affine interpolant of $(z^k)_{k=1,...,K}$ in the sense that $\widehat{z}_\tau(t_k) = z^k$ for $k = 0,...,K$. The estimate

$$\sup_{t \in [0,T]} ||z - \widehat{z}_\tau||_{\mathcal{A}}^2 \leq 4 \sum_{k=1}^{K} \tau_k \varepsilon_k + 4T \sum_{k=1}^{K} \tau_k^3 \sup_{t \in [t_{k-1}, t_k]} ||\dot{r}||_{\mathcal{A}}^2$$

holds with the nonnegative quantities

$$\varepsilon_k = \tau_k \langle A d_t z^k, r^k \rangle - \tau_k ||d_t z^k||_{\mathcal{A}}^2$$

for $k = 1,...,K$, where $\|\cdot\|_{\mathcal{A}}$ is the norm induced by the bilinear form $\mathcal{A}$.

Proof. The condition for z^k immediately implies $Az^k \in C_*$ as well as

$$\langle v - Az^k, -d_t z^k + r^k \rangle \leq 0$$

for all $v \in C_*$ and $k = 1,...,K$. Since $z^0 = z(0)$, the condition for z also yields $Az^0 \in C_*$ and we may choose $v = Az^{k-1}$ to find

$$-\varepsilon_k = \tau_k ||d_t z^k||_{\mathcal{A}}^2 - \tau_k \langle A d_t z^k, r^k \rangle \leq 0.$$

Let $z_\tau^+ : [0,T] \to Y$ denote the piecewise constant interpolant of (z^k) with $z_\tau^+(t) = z^k$ for $t \in (t_{k-1}, t_k]$. Similarly r_τ^+ is the piecewise constant interpolant of (r^k). For all $t \in [0,T]$ and $v \in C_*$ we have

$$\langle v - Az_\tau^+, -\partial_t \widehat{z}_\tau + r_\tau^+ \rangle \leq 0.$$

The definition

$$\rho_\tau = \langle Az_\tau^+ - A\widehat{z}_\tau, -\partial_t \widehat{z}_\tau + r_\tau^+ \rangle$$

leads to

$$\langle v - A\widehat{z}_\tau, -\partial_t \widehat{z}_\tau + r \rangle \leq \rho_\tau + \langle v - A\widehat{z}_\tau, r - r_\tau^+ \rangle.$$

Considering the condition for z, we also have

$$\langle v - Az, -\partial_t z + r \rangle \leq 0.$$

Choosing $v = Az$ and $v = A\widehat{z}_\tau$ in the last two inequalities respectively and adding them, we find that

$$\langle A(z - \widehat{z}_\tau), \partial_t(z - \widehat{z}_\tau) \rangle \leq \rho_\tau + \langle A(z - \widehat{z}_\tau), r - r_\tau^+ \rangle.$$

Using $\frac{d}{dt} \|w\|_{\mathcal{A}}^2 = 2\langle Aw, \partial_t w \rangle$ for $w \in Y$ as well as Cauchy-Schwarz and Young's inequality leads to the estimate

$$\frac{1}{2} \frac{d}{dt} \|z - \widehat{z}_\tau\|_{\mathcal{A}}^2 \leq \rho_\tau + T\|r - r_\tau^+\|_{\mathcal{A}}^2 + \frac{1}{4T} \|z - \widehat{z}_\tau\|_{\mathcal{A}}^2. \tag{5}$$

For $t \in [t_{k-1}, t_k]$ we can use $z_\tau^+ - \widehat{z}_\tau = -(t - t_k)d_t z^k$ to find

$$\rho_\tau = (t - t_k)\|d_t z^k\|_{\mathcal{A}}^2 - (t - t_k)\langle Ad_t z^k, r^k \rangle = \frac{t - t_k}{\tau_k}(-\varepsilon_k) \leq \varepsilon_k.$$

Let $t^* \in [0, T]$, so that the maximum of $t \mapsto \|z - \widehat{z}_\tau\|_{\mathcal{A}}$ is attained at t^*. We integrate inequality (5) over the interval $[0, t^*]$ and note that $\|r - r_\tau^+\|_{\mathcal{A}} \leq \tau_k \sup_{t \in [t_{k-1}, t_k]} \|\dot{r}\|_{\mathcal{A}}$ as well as $z(0) = z^0$ to show the estimate

$$\frac{1}{2} \sup_{t \in [0,T]} \|z - \widehat{z}_\tau\|_{\mathcal{A}}^2 \leq \sum_{k=1}^{K} \tau_k \varepsilon_k + T \sum_{k=1}^{K} \tau_k^3 \sup_{t \in [t_{k-1}, t_k]} \|\dot{r}\|_{\mathcal{A}}^2 + \frac{1}{4} \sup_{t \in [0,T]} \|z - \widehat{z}_\tau\|_{\mathcal{A}}^2,$$

which proves the theorem. $\qquad\square$

3. **Application to elastoplasticity.** The next step is to apply the general framework to the elastoplastic model problem and to formulate the error estimate in a way, that enables us to define a time adaptive algorithm. We assume homogeneous initial conditions and a combination of linear kinematic and isotropic hardening as well as the von-Mises flow rule. For a derivation of the model, we refer the reader to [6].

Consider a bounded Lipschitz domain $\Omega \subset \mathbb{R}^d$ with a closed, possibly empty set $\Gamma_D \subset \partial\Omega$ and let $H_D^1(\Omega)$ be the set of functions in $H^1(\Omega)$, that vanish on Γ_D. Additionally, let $\Gamma_N = \partial\Omega \setminus \Gamma_D$, a volume force $f \in W^{2,\infty}([0,T]; L^2(\Omega; \mathbb{R}^d))$ and a boundary force $g \in W^{2,\infty}([0,T]; L^2(\Gamma_N, \mathbb{R}^d))$.

The framework of Section 2 can be applied to plasticity by using the Hilbert space

$$Y = H_D^1(\Omega, \mathbb{R}^d) \times L^2(\Omega, \mathbb{R}_{\mathrm{sym}}^{d \times d}) \times L^2(\Omega)$$

as well as the mappings

$$\mathcal{A}(y, w) = \int_\Omega \mathbb{C}(\varepsilon(u) - p) : (\varepsilon(v) - q) + \mathbb{H}_{\mathrm{kin}}p : q + \mathbb{H}_{\mathrm{iso}}ae \; dx,$$

$$\langle \ell(t), w \rangle = \int_{\Gamma_N} g(t) \cdot v \; ds + \int_\Omega f(t) \cdot v \; dx, \tag{6}$$

$$\Psi(y) = \int_\Omega I_S^*(p, a) \; dx,$$

for $y = (u, p, a) \in Y$ and $w = (v, q, e) \in Y$. Here, $\mathbb{C} : \mathbb{R}_{\mathrm{sym}}^{d \times d} \to \mathbb{R}_{\mathrm{sym}}^{d \times d}$ with

$$\mathbb{C}B = 2\mu B + \lambda \operatorname{tr}(B)I_d$$

represents Hooke's law and makes use of the material specific Lamé parameters $\mu > 0$ and $\lambda > 0$. Furthermore, $\varepsilon(u)$ denotes the symmetric gradient of u and $\mathbb{H}_{\mathrm{kin}}, \mathbb{H}_{\mathrm{iso}} \geq 0$ are the hardening modules for kinematic and isotropic hardening respectively. Because of the assumed homogeneous initial conditions we are able to eliminate the inner variable b, that is commonly used for kinematic hardening, and have

$$I_S^*(p, a) = \begin{cases} \sigma_y |p| & \text{if } \operatorname{tr} p = 0 \text{ and } \sigma_y |p| \leq -a, \\ +\infty & \text{otherwise.} \end{cases}$$

The quantities of interest in this formulation are the displacement u, the plastic strain p, and an inner variable a, which measures the accumulation of isotropic hardening. The stress $\sigma = \mathbb{C}(\varepsilon(u) - p)$, that is commonly sought in dual or mixed formulations of the problem, only plays an implicit role in this case.

By applying Theorem 2.3, we conclude the estimate

$$\sup_{t \in [0,T]} ||z - \widehat{z}_\tau||_{\mathcal{A}}^2 \leq 4 \sum_{k=1}^K \tau_k \varepsilon_k + 4T \sum_{k=1}^K \tau_k^3 \sup_{t \in [t_{k-1}, t_k]} ||\dot{r}||_{\mathcal{A}}^2,$$

which provides us with an accessible bound for the error between a solution of the continuous problem and a solution of a semi-discrete problem in time. However, in order to be able to run numerical tests, an estimate for a fully discrete solution is required. Hence, we use a P_1-FEM to achieve the discretization in space.

We consider a regular triangulation $\mathcal{T}_h$ of Ω and let $\mathcal{S}_D^1(\mathcal{T}_h) \subset H_D^1(\Omega)$ be the set of continuous functions, that are affine on each element of $\mathcal{T}_h$ and vanish on Γ_D. Similarly, $\mathcal{L}^0(\mathcal{T}_h) \subset L^2(\Omega)$ contains functions, that are constant on each element of $\mathcal{T}_h$.

With these notations we define the Hilbert space

$$Y_h = \mathcal{S}_D^1(\mathcal{T}_h)^d \times \mathcal{L}^0(\mathcal{T}_h)_{\mathrm{sym}}^{d \times d} \times \mathcal{L}^0(\mathcal{T}_h),$$

which is a subspace of Y. By simply using Y_h in the Definitions 2.1 and 2.2, we obtain a semi-discrete problem in space and a fully discrete problem, both of which have unique solutions. The latter seeks $(u_h^k, p_h^k, a_h^k)_{k=1,\dots,K} \subset Y_h$, such that

$$\int_\Omega \mathbb{C}(\varepsilon(u_h^k) - p_h^k) : (\varepsilon(v_h - d_t u_h^k) - (q_h - d_t p_h^k)) \, dx$$

$$+ \int_\Omega \mathbb{H}_{\mathrm{kin}} p_h^k : (q_h - d_t p_h^k) + \mathbb{H}_{\mathrm{iso}} a_h^k (e_h - d_t a_h^k) \, dx$$

$$+ \int_\Omega I_S^*(q_h, e_h) \, dx - \int_\Omega I_S^*(d_t p_h^k, d_t a_h^k) \, dx$$

$$\geq \int_{\Gamma_N} g(t) \cdot (v_h - d_t u_h^k) \, ds + \int_\Omega f(t) \cdot (v_h - d_t u_h^k) \, dx$$

for all $(v_h, q_h, e_h) \in Y_h$ and $k = 1, \dots K$.

Similar to the linear operator A, we define $A_h : Y_h \to Y_h'$ via $\langle A_h v_h, w_h \rangle = \mathcal{A}(v_h, w_h)$ for $v_h, w_h \in Y_h$. Since the important properties of the maps in (6) remain valid on Y_h, we are still able to apply Theorem 2.3 and conclude the following corollary.

Corollary 1. *Suppose that $y_h : [0, T] \to Y_h$ and $(y_h^k)_{k=0,\dots,K} \subset Y_h$ are solutions of the space discrete and fully discrete problem respectively. Let $\widehat{y}_{\tau,h} : [0, T] \to Y_h$*

denote the piecewise affine interpolant of (y_h^k) with $\widehat{y}_{\tau,h}(t_k) = y_h^k$ for $k = 0, ..., K$. Similarly, $\widehat{\ell}_\tau$ is the interpolant of (ℓ^k). The estimate

$$\sup_{t \in [0,T]} ||y_h - \widehat{y}_{\tau,h}||_{\mathcal{A}}^2 \leq 8 \sum_{k=1}^{K} \tau_k \varepsilon_k + 2 \sup_{t \in [0,T]} ||A_h^{-1}(\ell - \widehat{\ell}_\tau)||_{\mathcal{A}}^2$$

$$+ 8T \sum_{k=1}^{K} \tau_k^3 \sup_{t \in [t_{k-1}, t_k]} ||A_h^{-1}(\partial_{tt}^2 \ell)||_{\mathcal{A}}^2$$

holds with

$$\varepsilon_k = \tau_k \int_{\Gamma_N} (d_t g(t_k)) \cdot d_t u_h^k \, ds + \tau_k \int_\Omega (d_t f(t_k)) \cdot d_t u_h^k \, dx$$

$$- \tau_k \int_\Omega \mathbb{C}(\varepsilon(d_t u_h^k) - d_t p_h^k) : (\varepsilon(d_t u_h^k) - d_t p_h^k) \, dx$$

$$- \tau_k \int_\Omega \mathbb{H}_{\text{kin}} d_t p_h^k : d_t p_h^k \, dx - \tau_k \int_\Omega \mathbb{H}_{\text{iso}} (d_t a_h^k)^2 \, dx$$

for $y_h^k = (u_h^k, p_h^k, a_h^k)$ and $k = 1, ..., K$.

Proof. Using the identities $z_h = -y_h + A_h^{-1}\ell$ and $z_h^k = -y_h^k + A_h^{-1}\ell^k$ as well as the triangle inequality and $(a+b)^2 \leq 2a^2 + 2b^2$, we find that

$$\sup_{t \in [0,T]} ||y_h - \widehat{y}_{\tau,h}||_{\mathcal{A}}^2 = \sup_{t \in [0,T]} ||\widehat{z}_{\tau,h} - z_h + A_h^{-1}(\ell - \widehat{\ell}_\tau)||_{\mathcal{A}}^2$$

$$\leq 2 \sup_{t \in [0,T]} ||z_h - \widehat{z}_{\tau,h}||_{\mathcal{A}}^2 + 2 \sup_{t \in [0,T]} ||A_h^{-1}(\ell - \widehat{\ell}_\tau)||_{\mathcal{A}}^2.$$

We apply Theorem 2.3 and note, that $r_h = A_h^{-1}\dot{\ell}$ to conclude the estimate. It remains to show the characterization of ε_k. We have

$$\langle A_h d_t z_h^k, A_h^{-1} d_t \ell^k \rangle = -\langle A_h d_t y_h^k, A_h^{-1} d_t \ell^k \rangle + \langle d_t \ell^k, A_h^{-1} d_t \ell^k \rangle$$

as well as

$$-||d_t z_h^k||_{\mathcal{A}}^2 = -\langle A_h d_t z_h^k, d_t z_h^k \rangle$$

$$= -||d_t y_h^k||_{\mathcal{A}}^2 + \langle d_t \ell^k, d_t y_h^k \rangle$$

$$+ \langle A_h d_t y_h^k, A_h^{-1} d_t \ell^k \rangle - \langle d_t \ell^k, A_h^{-1} d_t \ell^k \rangle.$$

We add the two equalities, multiply with τ_k and note, that $r^k = A_h^{-1} d_t \ell^k$ to obtain

$$\varepsilon_k = \tau_k \langle d_t \ell^k, d_t y_h^k \rangle - \tau_k ||d_t y_h^k||_{\mathcal{A}}^2.$$

The asserted characterization of ε_k follows from the definitions of $\mathcal{A}$ and ℓ displayed in (6). $\qquad\square$

Now that we control the error for our specific problem, the next goal is to establish $(\varepsilon_k)_{k=1,...,K}$ as refinement indicators for the implementation of time adaptivity. To accomplish this, we aim at identifying an estimate of the form

$$\sup_{t \in [0,T]} ||y_h - \widehat{y}_{\tau,h}||_{\mathcal{A}}^2 \leq \gamma \sum_{k=1}^{K} \tau_k \varepsilon_k, \tag{7}$$

where the last two terms on the right-hand side of the estimate from Corollary 1 are not present.

Remark 1. i) If the body force f and the boundary force g, and therefore the map ℓ, are linear with respect to the temporal variable t, the terms $\ell - \widehat{\ell}_\tau$ and $\partial^2_{tt}\ell$ vanish. In this case, the proofs of Theorem 2.3 and Corollary 1 can be simplified and we obtain the estimate

$$\sup_{t\in[0,T]} ||y_h - \widehat{y}_{\tau,h}||^2_{\mathcal{A}} \leq 2\sum_{k=1}^{K} \tau_k \varepsilon_k.$$

ii) Defining $\tau = \max\{\tau_k : k = 1, ..., K\}$, we are able to determine convergence rates for each individual term on the right-hand side of the estimate in Corollary 1. We have

$$\sum_{k=1}^{K} \tau_k \varepsilon_k \qquad\qquad\qquad \in O(\tau^2), \tag{8}$$

$$\sum_{k=1}^{K} \tau_k^3 \sup_{t\in[t_{k-1},t_k]} ||A_h^{-1}(\partial^2_{tt}\ell)||^2_{\mathcal{A}} \in O(\tau^2), \tag{9}$$

whereas the continuity of A_h^{-1} and a standard estimate for linear spline interpolation yield

$$\sup_{t\in[0,T]} ||A_h^{-1}(\ell - \widehat{\ell}_\tau)||^2_{\mathcal{A}} \in O(\tau^4), \tag{10}$$

see [4] for details. The lower convergence rates in (8) and (9) justify discarding term (10), if τ is small.

iii) Term (9) is predetermined by the applied forces f and g and does not depend on the computed solution. Therefore, it is possible to define regions, where the temporal grid needs to be refined, before a potential algorithm is even started. An alternative strategy is to merge the two remaining terms and define the new refinement indicator

$$\varepsilon'_k = \varepsilon_k + T\tau_k^2 \sup_{t\in[t_{k-1},t_k]} ||A_h^{-1}(\partial^2_{tt}\ell)||^2_{\mathcal{A}}$$

$$\leq \varepsilon_k + T\tau_k^2 c_{A_h} \sup_{t\in[t_{k-1},t_k]} ||\partial^2_{tt}\ell||^2_{Y'_h},$$

where c_{A_h} is an upper bound for the operator norm of A_h^{-1}.
However, since in all of our tests ℓ is linearly dependent on t and we know, that an additional refinement based on the second derivative of ℓ is possible, we will assume (7) for the rest of this paper.

It is important to note, that by approximating the semi-discrete solution in space, we basically isolate the error caused by the time discretization for our time adaptive algorithm to properly identify where to refine the temporal grid. The error introduced by the space discretization is therefore not taken into account here. However, as mentioned in the introduction, estimates and adaptive algorithms in space exist elsewhere.

4. **Time adaptive algorithm.** Now that $(\varepsilon_k)_{k=1,..K}$ are established as refinement indicators, we are able to formulate a time adaptive algorithm for the computation of a numerical solution to the elastoplastic problem. It makes use of the user defined parameters $\varepsilon_{\max}$, which defines an upper bound for the refinement indicators ε_k, and θ, which determines the grid coarsening strategy the algorithm follows.

Algorithm 1 (Adaptive time stepping). Let $k = 0$, $y_h^0 \in Y_h$, $t_0 = 0$, $\tau > 0$, $\varepsilon_{\max} > 0$ and $\theta \in [0,1]$.

1. Set $k \mapsto k+1$.
2. Set $t_k = t_{k-1} + \tau$.
3. If $t_k > T$, set $t_k = T$ and $\tau = T - t_{k-1}$.
4. Use an iterative solution method to compute the solution y_h^k for the time t_k.
5. Compute $\varepsilon_k(y_h^k)$.
6. If $\varepsilon_k > \varepsilon_{\max}$, set $\tau \mapsto \tau/2$ and continue with Step 2.
7. If $t_k = T$, stop the algorithm.
8. If $\varepsilon_k \leq \theta\varepsilon_{\max}$, set $\tau \mapsto 2\tau$.
9. Continue with Step 1.

Considering an adaptive algorithm it is important to distinguish the two main reasons for using it: reduction of stored data and reduction of computation time. The former is determined by the number of time steps K. The latter however depends on K_{tot}, the total number of computed steps. This includes the times, Steps 2-6 are taken, but need to be repeated with a smaller stepsize, because the refinement indicator ε_k was too large.

The conditions under which the algorithm attempts to coarsen the grid (Step 8) play an important role in reducing K and K_{tot}. This motivates the introduction of the parameter θ.

For $\theta = 1$ the algorithm doubles the stepsize after every successful time step. On the one hand, this will minimize K, because every opportunity to coarsen the grid will be taken. But on the other hand, if the error is relatively constant or increases with time, the stepsize will always have to immediately be reduced again, which leads to an increase of K_{tot}. In these cases, if a minimization of computation time is desired, a parameter $\theta \in (0,1)$ may be in order.

The case $\theta = 0$ should only be used, if the error never decreases, which means that the stepsize never needs to be increased. To decide this before starting the algorithm requires a high amount of a priori knowledge about the problem and its solution though.

Algorithm 1 is not specific to our a posteriori estimate or model problem. It can be used for time adaptivity in general by substituting ε_k with a refinement indicator, that was obtained from another estimate. However, as the proof of the following proposition indicates, we require uniform boundedness of ε_k/τ_k to ensure the termination of the algorithm.

Proposition 1. *Algorithm 1 terminates after a finite number of iterations.*

Proof. Using Cauchy-Schwarz and Young's inequality, we have

$$\frac{\varepsilon_k}{\tau_k} = \langle A_h d_t z^k, r^k \rangle - \|d_t z^k\|_{\mathcal{A}}^2$$

$$\leq \|d_t z^k\|_{\mathcal{A}} \|r^k\|_{\mathcal{A}} - \|d_t z^k\|_{\mathcal{A}}^2$$

$$\leq \frac{1}{4}\|r^k\|_{\mathcal{A}}^2.$$

We note, that $r^k = A_h^{-1} d_t \ell^k$ and $\|A_h^{-1} d_t \ell^k\|_{\mathcal{A}} \leq \sup_{t\in[0,T]} \|A_h^{-1}\dot{\ell}\|_{\mathcal{A}}$, which leads to

$$\frac{\varepsilon_k}{\tau_k} \leq \frac{1}{4} \sup_{t\in[0,T]} \|A_h^{-1}\dot{\ell}\|_{\mathcal{A}}^2 =: M.$$

Employing the continuity of A_h^{-1}, we can see, that the regularity condition $\ell \in W^{2,\infty}([0,T;Y'])$, that was required for Theorem 2.3, is more than enough to ensure the uniform boundedness of ε_k/τ_k.

Let $\tau_\varepsilon := M^{-1}\varepsilon_{\max}$ and consider $0 < \tau_k \leq \tau_\varepsilon$. Since M is a uniform upper bound for ε_k/τ_k we have

$$\varepsilon_k = \tau_k \frac{\varepsilon_k}{\tau_k} \leq \tau_\varepsilon M = \varepsilon_{\max}.$$

This means, that whenever the stepsize τ_k is smaller than τ_ε, the corresponding refinement indicator ε_k is smaller than $\varepsilon_{\max}$. Therefore, the algorithm will proceed with the next time step and not decrease the stepsize any further. Since we only change the stepsize by multiplying or dividing it by 2, a lower bound for τ_k is $\tau_\varepsilon/2$. The algorithm thus terminates after a maximum of

$$K_{\max} = \lceil 2\tau_\varepsilon^{-1}T \rceil = \lceil 2MT\varepsilon_{\max}^{-1} \rceil$$

time steps. $\qquad\qquad\qquad\qquad\qquad\qquad\qquad\qquad\qquad\qquad\qquad\qquad\qquad\qquad$ $\square$

Remark 2. Related time-stepping algorithms have been proposed for the linear heat equation. In that case termination results for coupled space-time adaptive strategies have been proved in [7].

5. **Numerical tests.** In this section we report on numerical experiments to verify that Algorithm 1 actually improves the error estimate when compared to a method with constant stepsize. Our implementation of elastoplasticity is based on a displacement formulation of the problem. It states that if the displacement u_h^k for the current time t_k is known, the remaining variables can be computed via

$$d_t p_h^k = \frac{\left(|\xi| - \sigma_y(1 - \mathbb{H}_{\mathrm{iso}}a_h^{k-1})\right)_+}{2\tau_k(\mu + \mathbb{H}_{\mathrm{iso}}\sigma_y^2 + \mathbb{H}_{\mathrm{kin}})}\frac{\xi}{|\xi|} \qquad \text{and} \qquad d_t a_h^k = -\sigma_y|d_t p_h^k|,$$

where

$$\xi = \mathrm{dev}\left(\mathbb{C}(\varepsilon(u_h^k) - p_h^{k-1}) - \mathbb{H}_{\mathrm{kin}}p_h^{k-1}\right) \qquad \text{and} \qquad \mathrm{dev}(B) = B - \frac{1}{d}\mathrm{tr}(B)I_d.$$

Additionally, we want to compute u_h^k, such that

$$\int_\Omega \left(\mathbb{C}(\varepsilon(u_h^k) - p_h^{k-1}) - \tau_k\mathbb{C}d_t p_h^k\right) : \nabla v_h\, dx = \int_\Omega f(t_k)\cdot v_h\, dx + \int_{\Gamma_N} g(t_k)\cdot v_h\, ds$$

holds for all $v_h \in \mathcal{S}_D^1(\mathcal{T}_h)^d$. However, due to the nonlinear nature of this equation, we employ a Newton iteration to obtain u_h^k. A super linear convergence property of the employed Newton iteration has been established in [16]. For more information about the implementation we refer the reader to [1] or [4].

For simplification purposes we restrict the model to vanishing volume forces and linear kinematic hardening, i.e. we set $f \equiv 0$ and the constants $\mathbb{H}_{\mathrm{kin}} = 1$ and $\mathbb{H}_{\mathrm{iso}} = 0$. Additionally, the yield stress $\sigma_y = 243$ as well as the Lamé parameters $\mu = \frac{E}{2(1+\nu)}$ and $\lambda = \frac{\nu E}{(1+\nu)(1-2\nu)}$ with $E = 70000$ and $\nu = 0,33$ are used. The first problem we consider for our tests is a radially loaded ring.

Example 1 (Loaded ring). Consider $T = 16$, $\Omega = \{x \in \mathbb{R}^2 | \ 1 < \sqrt{x_1^2 + x_2^2} < 2\}$ and $g_r : [0, T] \to \mathbb{R}^+$ with $g_r(t) = 4\sqrt{3/2}t$. The Neumann boundary conditions

$$g(x, t) = \begin{cases} 4g_r(t)\frac{x}{|x|} & \text{for } |x| = 1, \\ -g_r(t)\frac{x}{|x|} & \text{for } |x| = 2, \end{cases}$$

apply on $\Gamma_N = \partial\Omega$.
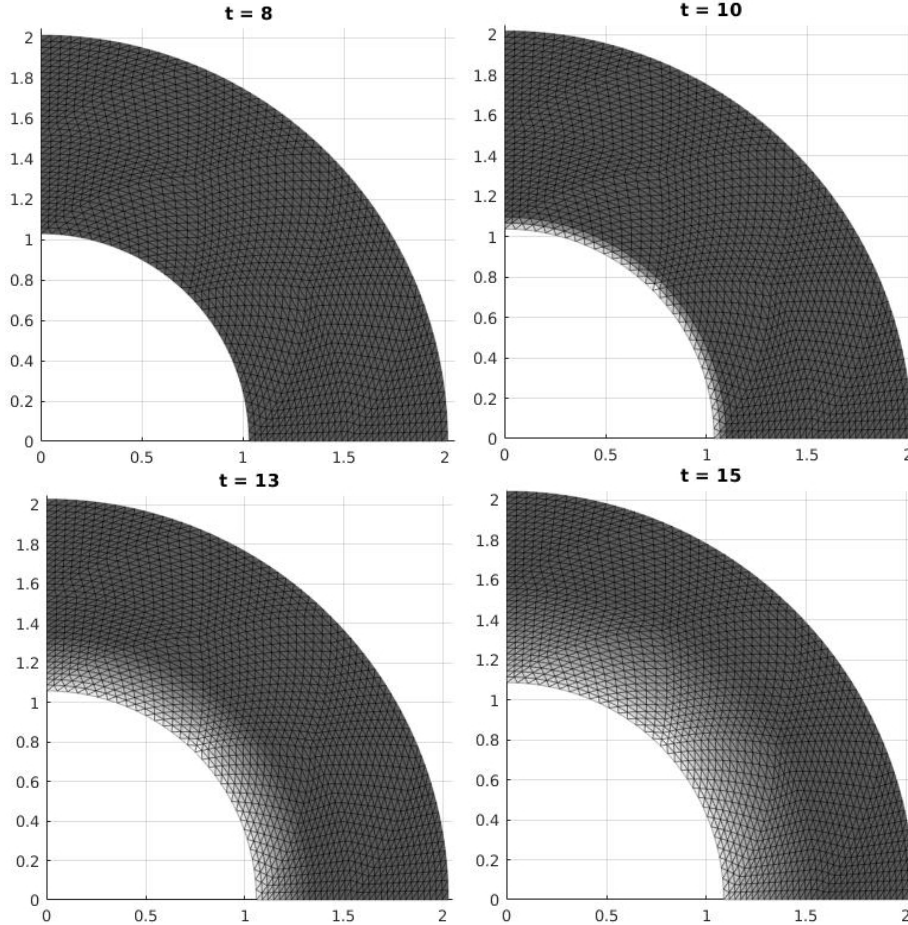
FIGURE 1. Numerical approximation of the solution for Example 1 at times $t = 8, 10, 13, 15$. The grey shading corresponds to the norm of plastic strain p. For visibility purposes, we only applied 4 red refinements as opposed to our actual tests, where 6 red refinements were used. The radially symmetric nature of the problem allows us to save computation time by only computing the solution for a quarter of the ring.

An analytical solution to this problem can be found in [2]. Figure 1 shows an approximation of the development of plastic strain p, that was obtained by using the method and parameters mentioned above. We see that plastic strains start to occur at the inner boundary of the ring, after which it begins to spread outwards.
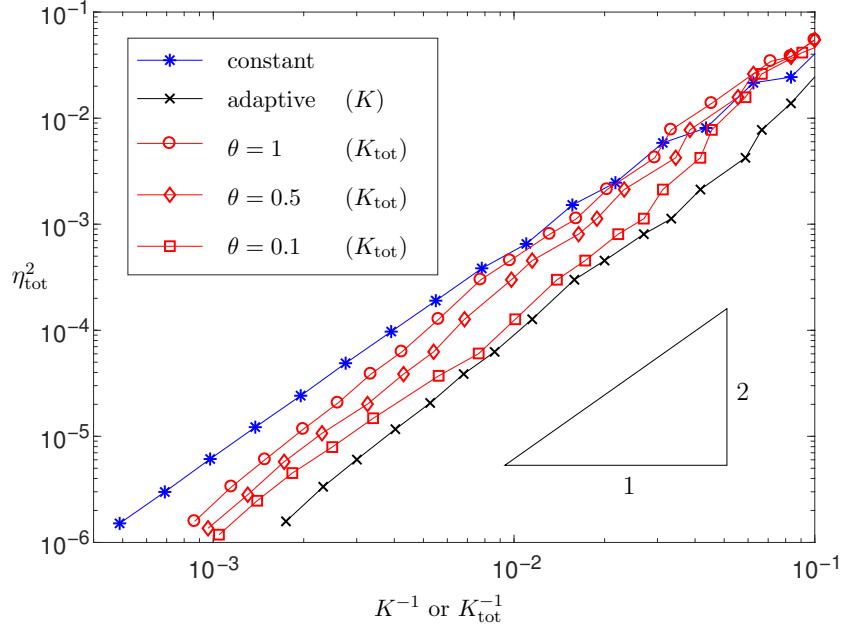
FIGURE 2.   Results of the tests using Example 1. Logarithmic plot of the error term η_{tot}^2 as a function of $K^{-1} \sim \tau$ for the method with constant time steps (star) and the adaptive algorithm with $\theta = 1$ (cross). The remaining graphs (circle, diamond and square) consider the total number of computed steps K_{tot} instead of the number of time steps K and show the results for different values of θ (see Algorithm 1). In the case of constant time steps, we have $K = K_{\text{tot}}$. The triangle in the bottom right references the slope of a quadratic function. An error reduction by the adaptive method is observed. The difference is less significant when considering K_{tot}, but increases for smaller values of θ.

As a reference point to compare our adaptive method to, we first run the tests with constant stepsizes $\tau = 2^{-\ell/2}$ for $\ell = 0, \ldots, 17$. To measure the approximation error, we resort to (7) and compute the term

$$\eta_{\text{tot}}^2 = \sum_{k=1}^{K} \tau_k \varepsilon_k.$$

Our next step is to employ Algorithm 1 with $\tau_{\text{start}} = 1$, $\varepsilon_{\max} = 10^{-n/4}$ for $n = 1, \ldots, 25$ and $\theta = 1$. The results of these tests can be seen in Figure 2 where the two methods are directly compared regarding the number of time steps K and the error term η_{tot}^2. Clearly, the adaptive method provides superior results for this problem in the sense that less time steps are required to obtain a similarly low approximation error.

Even if we compare computation time, and thus also account for the computed steps, where the refinement indicator ε_k was too high, (which is also shown in Figure 2,) we observe that the adaptive method still outperforms its counterpart for small stepsizes. In the context of this specific problem, the red lines additionally

indicate, that further improvement with a lower value of θ is possible. To see, if these results are specific to Example 1, we consider two further problems.

Example 2 (Elastoplastic fissure)**.** Let $T = 10$, $\Omega = (0,3) \times (0,1)$ and $g_2 : [0,T] \to \mathbb{R}$ with $g_2(t) = -4\sqrt{3/2}\,t$. The boundary of Ω is split into $\Gamma_D = [2,3] \times \{0,1\} \cup \{3\} \times [0,1]$ and $\Gamma_N = \partial\Omega \setminus \Gamma_D$. At $[0,2) \times \{1\} \subset \Gamma_N$, the condition $g = (0,g_2)^\top$ is applied, whereas homogeneous Neumann and Dirichlet boundary conditions hold on the rest of Γ_N and Γ_D respectively.

In Example 2 we think of the domain Ω as the cross section of a bar of metal, that is fixed by a vice on one side, while a growing force is applied from above, see Figure 3. Figure 4 shows, that a fissure develops between the fixed part and the free part of Ω, an ananalytical solution is not available.
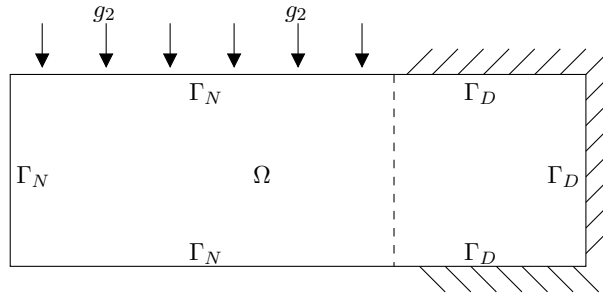
FIGURE 3. Illustration of the geometry used in Example 2.
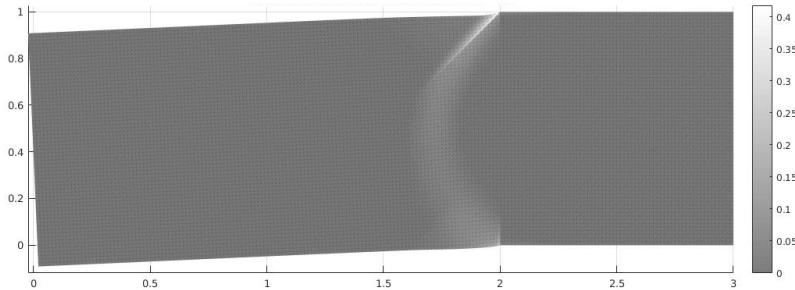
FIGURE 4. Numerical approximation of the solution for Example 2 at time $T = 10$. The original triangulation of three halved squares was red refined 6 times and the grey shading corresponds to the norm of plastic strain p. The increasing force causes a curved fissure to develop across the domain.

Example 3 (Uniform compression)**.** Consider $T = 200$, $\Omega = (0,2) \times (0,1)$ and $g_2 : [0,T] \to \mathbb{R}$ as in Example 2. We apply the Neumann boundary condition $g = (0,g_2)^\top$ at $\Gamma_N = (0,2) \times \{1\}$ and homogeneous Dirichlet boundary conditions at $\Gamma_D = [0,2] \times \{0\}$. On the sides $\{0,2\} \times (0,1)$ of Ω, symmetric boundary conditions are used, i.e. $u_1 = 0$ and $(\sigma_{21}, \sigma_{22}) \cdot n = 0$ with $\sigma = \mathbb{C}(\varepsilon(u) - p)$ and the outer unit normal n.
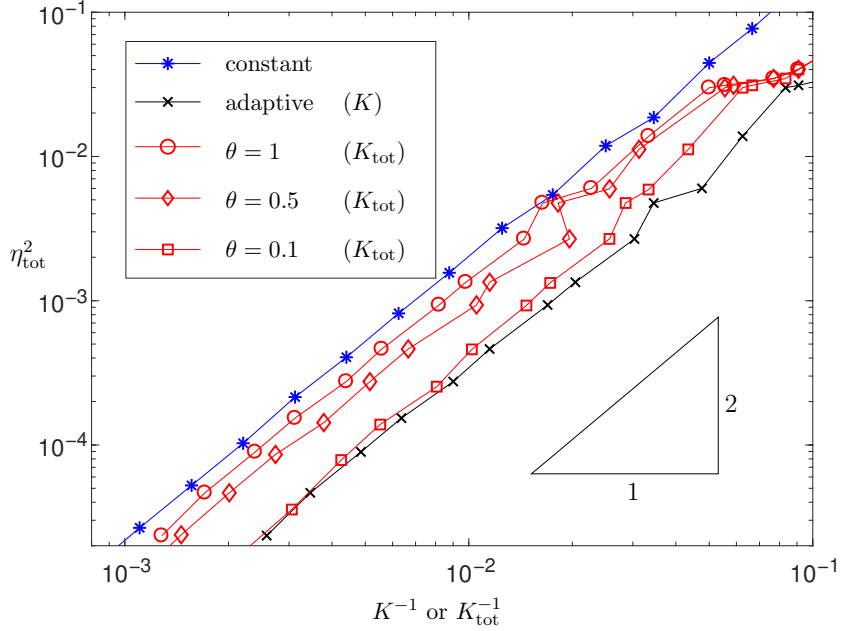
FIGURE 5. Results of the tests for Example 2 using notation from
Figure 2. The adaptive time stepping leads to an error reduction.

Example 3 models the deformations of the cross section of an infinitely long bar
of metal, that lies on the ground, while a growing force is applied from above. The
advantage of this problem is, that it is comparably easy to determine its analytical
solution. Additionally, this solution is simple in the sense, that p does not depend
on the space variable x. In other words, for a fixed time t, the plastic strain is
constant in Ω.
We are also able to determine the time t_p, when plastic strain simultaneously occurs
in all of Ω, by computing the root of the function $h(t) = \frac{1}{\sqrt{2}} \left(1 - \lambda/(2\mu + \lambda)\right) g_2(t) -$
σ_y. With our choices of g_2 and the material parameters, this yields $t_p \approx 138.32$.
Similar to our approach in Example 1, tests are run for the newly introduced prob-
lems and their results shown in Figure 6.
    Comparing all the tests, we observe that most of the general trends are consistent.
For similar amounts of steps,the adaptive algorithm always yields smaller error
terms than the method with constant steps, even if all computed steps are taken
into account.
While the tests on the first two problems yield fairly similar results, there are two
main distinctions between them and Example 3.

1. *The extent to which the adaptive method outperforms the ordinary one.* For
   Examples 1 and 2, the error term of the adaptive algorithm is not more than
   about 10 times smaller than for the method with constant steps. Testing with
   Example 3 however, this factor exceeds 10^4 for small time steps.
2. *The effect of modifying the parameter θ.* A lower value of θ reduces the amount
   of unnecessarily computed steps, when testing with Examples 1 and 2. This
   is not the case for Example 3.
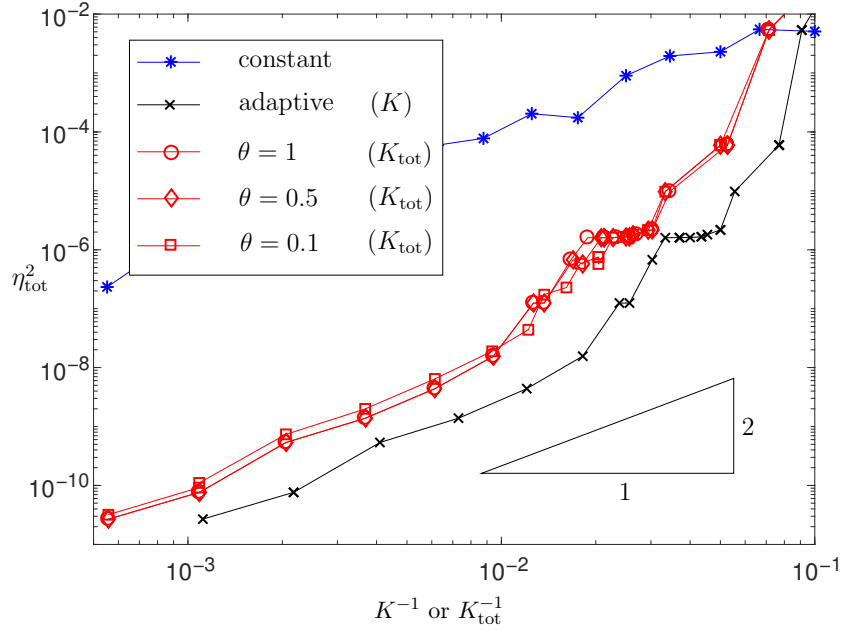
FIGURE 6. Results of the tests for Example 3 using notation from Figure 2. A stronger improvement of adaptity is observed than in Examples 1 and 2.

To understand why these differences occur, we look at the development of refinement indicator ε_k over time. To this end, we introduce the piecewise constant interpolant $\varepsilon_\tau : [0, T) \to \mathbb{R}^+$ with $\varepsilon_{\tau|[t_{k-1}, t_k)} = \varepsilon_k$ for all $k = 1, ..., K$. We are interested in this function because of the property

$$\int_0^T \varepsilon_\tau \; dt = \sum_{k=1}^K \tau_k \varepsilon_k = \eta_{\text{tot}}^2.$$

Figure 7 shows ε_τ as a function of t for the different examples. We observe, that ε_τ develops fairly similarly in the first two examples. There is a long period, where the error indicator is close to zero, after which it begins to monotonically increase. In Example 3 however, almost all the error potential is concentrated in the time interval, where plastic strain first emerges (see above). With these observations, we are able to explain both the differences between problems listed above.

The adaptive algorithm refines the time grid in regions of high values of ε_τ. Thus, to attain a low error during the later parts of Examples 1 and 2, a lot of time steps are required. For the last example on the other hand, the adaptive method only refines just before t_p, while in the rest of the time interval, the grid remains as coarse as possible with almost no negative effect on the error. In more general terms, adaptive methods are most effective, when used on problems with singularities and gradually lose their advantage, if the error potential is more evenly distributed.

The reason for different effects when modifying θ were basically already explained in Section 4. A value $\theta < 1$ means that the algorithm will sometimes not double the stepsize after a successful step. This is a positive change, if the error potential monotonically increases, e.g. in Examples 1 and 2, because the change in stepsize
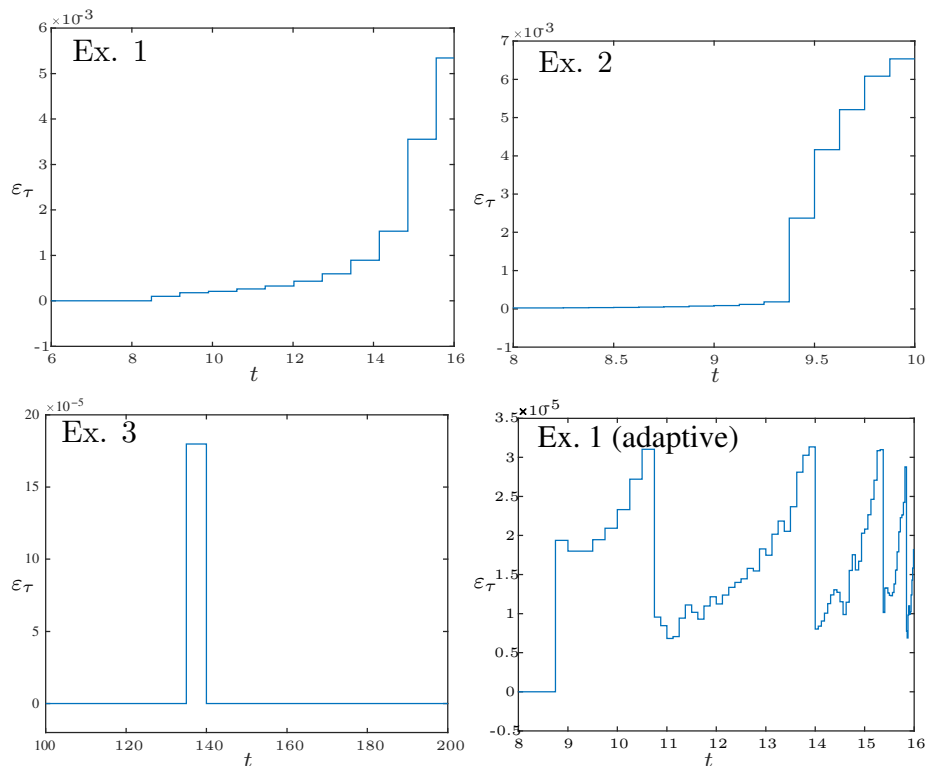
FIGURE 7. Development of error function ε_τ in time. The algorithm with constant time steps was used on Examples 1 (top-left), 2 (top-right) and 3 (bottom-left). The plot on the bottom-right shows the adaptive method for Example 1 and with $\varepsilon_{\max} = 3.16 \cdot 10^{-5}$. The graphs start at $t > 0$, because the error in the left out parts is almost zero. Similar results are observed for Examples 1 and 2, where after a certain amount of time, ε_τ starts to monotonically increase. In Example 3, a single peak occurs during the step containing the time $t_p \approx 138.32$, when plastic strain first emerges.

would immediately have to be reverted anyway. For Example 3 however, the ability to quickly increase the stepsize should be maintained in order to coarsen the grid after t_p.

Our observations indicate, that a priori knowledge about the particular problem is helpful to use the adaptive method optimally. It is possible to run an algorithm with a constantly high stepsize to obtain information about the error distribution without too much time investment. Based on these findings, an informed decision, if and how to use the adaptive algorithm, can be made.

Going back to Figure 7 once more, we are able to obtain additional insight into what causes a high error term at a specific point in time. Example 3 shows, that the occurrence of plastic strain does not necessarily lead to a large indicator ε_τ, because for $t > t_p$, the error term is relatively small. The peak at t_p rather indicates, that the initial occurrence of plastic strain, where the material switches from purely

elastic to elastoplastic behaviour, is the main reason for a large error term. This theory is supported by the fact, that in the other two problems, where plastic strain does not initially occur everywhere in Ω at the same time, the error is more spread out. Knowledge about this effect may be helpful when the general behaviour of a given problem is already known, but the computation method for an approximation remains to be chosen.

Our numerical experiments have confirmed, that for the elastoplastic problem with kinematic hardening, time adaptivity can be used to reduce the error introduced by the time discretization, while maintaining a similar computation time. To further decrease the number of computed steps, it is possible to change the conditions under which the algorithm increases the stepsize. However, the adaptive method does not improve convergence rates in the considered experiments and its effectiveness is heavily dependent on the specific problem at hand.
Additionally, when computing numerical solutions in plasticity, several approximation errors, that were not taken into account in this paper, may occur, e.g. resulting from space discretization or iterative solutions of the nonlinear problems. In practice, the different errors should thus be weighed against each other and the method chosen accordingly. It appears attractive to further combine the time adaptive algorithm with a space adaptive method.

REFERENCES

[1] J. Alberty, C. Carstensen, S. A. Funken, and R. Klose, *Matlab implementation of the finite element method in elasticity*, Computing **69** (2002), no. 3, 239–263.

[2] J. Alberty, C. Carstensen, and D. Zarrabi, *Adaptive numerical analysis in primal elastoplasticity with hardening*, Computer Methods in Applied Mechanics and Engineering **171** (1999), no. 3–4, 175–204.

[3] S. Bartels, *Quasi-optimal Error Estimates for Implicit Discretizations of Rate-Independent Evolutions*, SIAM Journal on Numerical Analysis **52** (2014), no. 2, 708–716.

[4] S. Bartels, *Numerical Methods for Nonlinear Partial Differential Equations*, Springer Series in Computational Mathematics, vol. 47, Springer, 2015.

[5] L. Gallimard, P. Ladevèze, and J. P. Pelle, *Error Estimation and Adaptivity in Elastoplasticity*, International Journal for Numerical Methods in Engineering **39** (1996), no. 2, 189–217.

[6] W. Han and B.D. Reddy, *Plasticity: Mathematical Theory and Numerical Analysis*, Interdisciplinary Applied Mathematics, Springer, 1999.

[7] C. Kreuzer, C. A. Möller, A. Schmidt, and K. G. Siebert, *Design and convergence analysis for an adaptive discretization of the heat equation*, IMA J. Numer. Anal. **32** (2012), no. 4, 1375–1403.

[8] D. Knees, *On global spatial regularity in elasto-plasticity with linear hardening*, Calc. Var. Partial Differential Equations **36** (2009), no. 4, 611–625.

[9] A. Mielke, *Evolution of rate-independent systems*, Handbook of Differential Equations: Evolutionary Equations **II** (2005), 461–559.

[10] A. Mielke and T. Roubíček, *Rate-Independent Systems: Theory and Applications*, Applied Mathematical Sciences, vol. 193, Springer, 2015.

[11] R. H. Nochetto, G. Savaré, and C. Verdi, *A posteriori error estimates for variable time-step discretizations of nonlinear evolution equations*, Communications on Pure and Applied Mathematics **53** (2000), no. 5, 525–589.

[12] S. I. Repin and J. Valdman, *Functional a posteriori error estimates for incremental models in elasto-plasticity*, Cent. Eur. J. Math. **7** (2009), no. 3, 506–519.

[13] J.C. Simo and T.J.R. Hughes, *Computational Inelasticity*, Interdisciplinary Applied Mathematics, Springer, 1998.

[14] G. Starke, *An Adaptive Least-Squares Mixed Finite Element Method for Elasto-Plasticity*, SIAM Journal on Numerical Analysis **45** (2007), no. 1, 371–388.

[15] U. Stefanelli, *A variational principle for hardening elastoplasticity*, SIAM J. Math. Anal. **40** (2008), no. 2, 623–652.

[16] M. Sauter and C. Wieners, *On the superlinear convergence in computational elasto-plasticity*, Comput. Methods Appl. Mech. Engrg. **200** (2011), no. 49-52, 3646–3658.

[17] A. Schröder and S. Wiedemann, *Error estimates in elastoplasticity using a mixed method*, Appl. Numer. Math. **61** (2011), no. 10, 1031–1045.

E-mail address: bartels@mathematik.uni-freiburg.de
E-mail address: jakob.keck92@gmx.de